The Effect of Moonlight on Observation of Cloud Cover at Night, and Application to Cloud Climatology

CAROLE J. HAHN*

Cooperative Institute for Research in Environmental Sciences, University of Colorado, Boulder, Colorado

STEPHEN G. WARREN

Department of Atmospheric Sciences, University of Washington, Seattle, Washington

JULIUS LONDON

Department of Astrophysical, Planetary, and Atmospheric Sciences, University of Colorado, Boulder, Colorado

(Manuscript received 5 November 1992, in final form 7 October 1994)

ABSTRACT

Visual observations of cloud cover are hindered at night due to inadequate illumination of the clouds. This usually leads to an underestimation of the average cloud cover at night, especially for the amounts of middle and high clouds, in climatologies based on surface observations. The diurnal cycles of cloud amounts, if based on all the surface observations, are therefore in error, but they can be obtained more accurately if the nighttime observations are screened to select those made under sufficient moonlight.

Ten years of nighttime weather observations from the Northern Hemisphere in December were classified according to the illuminance of moonlight or twilight on the cloud tops, and a threshold level of illuminance was determined, above which the clouds are apparently detected adequately. This threshold corresponds to light from a full moon at an elevation angle of 6°, light from a partial moon at higher elevation, or twilight from the sun less than 9° below the horizon. It permits the use of about 38% of the observations made with the sun below the horizon.

The computed diurnal cycles of total cloud cover are altered considerably when this moonlight criterion is imposed. Maximum cloud cover over much of the ocean is now found to be at night or in the morning, whereas computations obtained without benefit of the moonlight criterion, as in our published atlases, showed the time of maximum to be noon or early afternoon in many regions. Cloud cover is greater at night than during the day over the open oceans far from the continents, particularly in summer. However, near-noon maxima are still evident in the coastal regions, so that the global annual average oceanic cloud cover is still slightly greater during the day than at night by 0.3%. Over land, where daytime maxima are still obtained but with reduced amplitude, average cloud cover is 3.3% greater during the daytime. The diurnal cycles of total cloud cover we obtain are compared with those of ISCCP for a few regions; they are generally in better agreement if the moonlight criterion is imposed on the surface observations.

Using the moonlight criterion, we have analyzed 10 years (1982–91) of surface weather observations over land and ocean, worldwide, for total cloud cover and for the frequency of occurrence of clear sky, fog, and precipitation. The global average cloud cover (average of day and night) is about 2% higher if the moonlight criterion is imposed than if all observations are used. The difference is greater in winter than in summer, because of the fewer hours of darkness in summer. The amplitude of the annual cycle of total cloud cover over the Arctic Ocean and at the South Pole is diminished by a few percent when the moonlight criterion is imposed.

The average cloud cover for 1982–91 is found to be 55% for Northern Hemisphere land, 53% for Southern Hemisphere land, 66% for Northern Hemisphere ocean, and 70% for Southern Hemisphere ocean, giving a global average of 64%. The global average for daytime is 64.6%; for nighttime 63.3%.

1. Introduction

The diurnal cycles of total cloud cover and cloud-type amounts are of importance for understanding the earth's radiation budget, because cloud radiative forcing (Ramanathan et al. 1989; Harrison et al. 1990) is generally negative in the daytime but positive at night. Estimates of the climatological diurnal cycle can be made from surface observations as well as from satellite

* Current affiliation: Department of Atmospheric Sciences, University of Washington, Seattle, Washington.

Corresponding author address: Stephen G. Warren, Department of Atmospheric Sciences, AK-40, University of Washington, Seattle, WA, 98195.
E-mail: sgw@atmos.washington.edu

observations. The diurnal cycle obtained from satellite observations is subject to bias if the methods used to detect clouds are different during the day than at night. The diurnal cycle in surface-based climatologies can also be biased, because visual cloud observations by human observers are less accurate at night. The latter error is usually an underestimate, as shown by Sverdrup (1933, Fig. 107) in the Arctic, Riehl (1947) in the Atlantic, and Schneider et al. (1989) at the South Pole, all of whom sorted the observations according to the phase of the moon at particular geographical locations. Circumstantial evidence for such a "night-detection bias" was found by Warren et al. (1986, 1988) for middle and high clouds, but such a bias was not apparent for low clouds.

We have published atlases of the global distribution of total cloud cover and cloud-type amounts from surface observations covering 11 yr (1971–81) over land (Warren et al. 1986, hereafter W86) and 30 yr (1952–81) over the ocean (Warren et al. 1988, hereafter W88). In the analysis for total cloud cover and low cloud types we used all observations, regardless of the time of day, but because of the night-detection bias we used only "daytime" observations (0600–1800 local time) for middle and high clouds except in the polar regions. We therefore did not report diurnal cycles for the amounts of middle and high clouds. The atlases covered a span of years ending with 1981. We have now analyzed the subsequent 10 years, 1982–91, for total cloud cover and for the frequency of occurrence of clear sky, precipitation, and fog (Hahn et al. 1994). As part of that analysis, we developed a procedure to eliminate or greatly reduce the night-detection bias, which is described in this paper.

2. Visual cloud observations classified according to illumination

a. Data source

Surface weather observations were obtained from the National Meteorological Center for land stations and from the Comprehensive Ocean–Atmosphere Data Set (Woodruff et al. 1987) for ships. Synoptic weather reports are made eight times daily, at UTC hours divisible by 3. Substantially more ships report at the 6-h times (0000, 0600, 1200, 1800 UTC) than at the intermediate 3-h times. Land stations generally report every 3 h (except in the United States, Canada, and Australia, where most stations report only every 6 h), but some land stations report only during daytime.

The latitude belt 0°–50°N was used to study the effect of moonlight because it is the region of greatest data density and it spans latitudes with different cloud amounts, cloud types, and maximum lunar altitudes. The region was divided into five 10° zones for analysis. Land and ocean data were analyzed separately for the 10-yr period December 1981–November 1991. Results are presented here for the month of December (1981–90) for which the altitude of the full moon at midnight reaches maximum values in the higher latitudes of the Northern Hemisphere.

b. Illumination by the moon

Because we are studying visual observations, we use not radiometric units but rather photometric units (McCartney 1976, Chapter 1), which consider only visible wavelengths and take into account the spectral response of the eye. We compute the illuminance on a horizontal surface at the top of the atmosphere (TOA) and assume that the variation in illuminance (the photometric analogue of irradiance) due to lunar elevation is the same at the top of the cloud as at TOA. We therefore neglect all atmospheric absorption (which would be different above low clouds than above high clouds); this is a minor effect compared with the variations of illuminance due to lunar phase, elevation, and distance. We also do not account for variations in atmospheric scattering above the different levels of clouds, because much of the scattered light is not lost to space but is scattered down and therefore contributes to the illumination of the clouds.

We define a "relative lunar illuminance" R at the top of the atmosphere as

$$R = \Phi \sin h_m (\bar{r}^2/r^2), \qquad (1)$$

where h_m is the lunar altitude (angle of the moon above the horizon), r is the earth–moon distance, and $\bar{r}$ its mean value. For r we use the "topocentric" distance, that is, from locations on the earth's surface rather than from the center of the earth. The value of r^2 varies by about ±15% from its mean because of the eccentric lunar orbit. The term Φ is the lunar phase function described below; its value varies between 0.0 and 1.0. The relative illuminance R obtains a value of 1.0 when the full moon is overhead at its mean distance from the earth. For our data of 10 Decembers the maximum value of R was 1.18. A negative value of R means the moon is below the horizon.

The lunar phase function Φ (as distinct from the scattering phase function used in radiative transfer theory) is the average brightness of the lunar surface, as seen from the earth, relative to its maximum value that would occur for a full moon at a phase angle of zero if the moon were not eclipsed. (The phase angle is the angle between sun and earth, as seen from the moon.) The measurements and theoretical explanation of the lunar phase function were reviewed by Hapke (1963, 1971); the data of Rougier (1933), cited by Hapke, are reproduced here as the dashed lines in Fig. 1. The data were obtained by a photoelectric cell sensitive to wavelengths of 390–550 nm (Fig. 13 of Rougier 1933). It is important to note that Φ is far from linear with phase angle α; the half moon (at first or third quarter; $\alpha = 90°$) is only one-tenth as bright as the full moon.

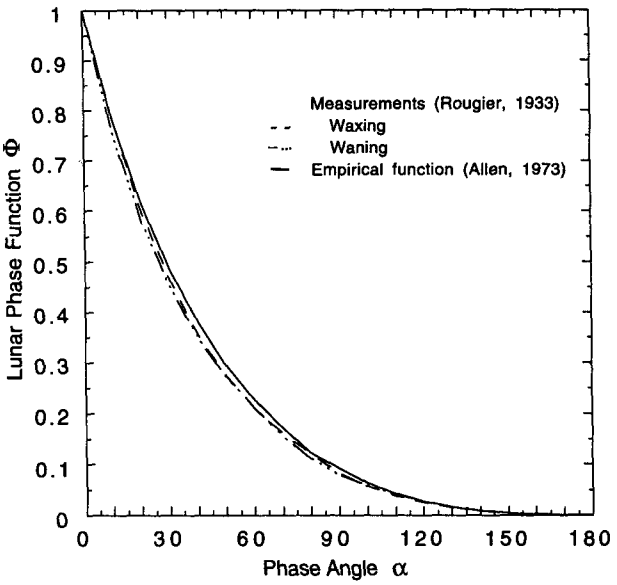

FIG. 1. Integral phase function of the moon (relative brightness, averaged over the lunar surface, as seen from the earth) from the experimental data of Rougier (1933), as quoted by Hapke (1963, 1971), and the empirical fit of Allen (1973, page 144). The phase angle α is the angle between the sun and the earth, as seen from the moon.

The phase function in Fig. 1 appears to differ from that given by Bond and Henderson (1963), reproduced by the Radio Corporation of America (1974), and used by Schneider et al. (1989) for classifying cloud observations at the South Pole. However, the two functions are actually not in disagreement because Bond and Henderson plotted relative illuminance as a function of elongation angle rather than phase angle. Elongation angle is the difference between the longitudes of sun and moon, so it varies through the entire range between 0° and 360° during a month, whereas the phase angle α goes to zero only during a lunar eclipse and in many months does not drop much below 5° because the moon's orbit is inclined by about 5° to the ecliptic plane. Bond and Henderson's value at an elongation angle of 180° (Fig. 6-3 of RCA 1974) is therefore a weighted average for phase angles 0°–5°.

Figure 1 shows that the waxing moon is slightly brighter than the waning moon at the same phase angle. We ignore this difference and for convenience use a simple analytical function given by Allen (1973, page 144) as an empirical fit to the data and shown as the solid line in Fig. 1, which approximately fits Rougier's observations:

$$-100^{1/5} \log_{10}\Phi = 0.026\alpha + 4.0 \times 10^{-9}\alpha^4, \quad (2)$$

where $0° \leq \alpha \leq 180°$. Allen's equation is written in this form such that the left-hand side represents the change in visual magnitude from that at zero phase angle. A unit change in visual magnitude is defined as a change in brightness by the fifth root of 100, or 2.512.

c. *Definition of "night"*

To quantify the effect of moonlight on cloud observations, we require a set of observations in which other sources of light (i.e., twilight) are negligible. Our own visual observations of clouds at night suggested that the twilight illumination was useful for cloud detection until the sun sank to 8°–9° below the horizon. To eliminate any possible influence of twilight, we therefore performed the initial analysis only on observations made when the sun was more than 12° below the horizon. The analysis (as described below) resulted in a threshold of moonlight above which clouds could be readily detected; this threshold illuminance could also be obtained from twilight with a solar altitude $h_s \approx -9°$. We then repeated the moonlight analysis on a larger set of nighttime observations, those with $h_s < -9°$. The results of the latter analysis are the ones presented here. For convenience we use the shorthand labels "night" for observations made with $h_s < -9°$, "twilight" for $-9° \leq h_s < -0.25°$ (because the angular width of the sun is 0.5°), and "daylight" for $-0.25° \leq h_s \leq 90°$.

d. *Data analysis*

The contents of surface weather reports and our method of error checking are described in W86. Total cloud cover is encoded in the report in eighths, with 0 representing clear sky and 8 representing overcast. For each report of the study period, the value of R is computed, given the date, time, latitude, and longitude of the report. The values of h_s, required for identification of "night," and of h_m, r, and α, required for Eqs. (1) and (2), were determined with the aid of an ephemeris in the form of a Fortran program written by Stephenson (1991, personal communication). The program actually gives latitude and longitude of sun and moon, from which we derive α, and lunar semidiameter in degrees, from which we derive r.

For each 10° latitude zone from 0° to 50°N, cloud data were sorted into 13 bins based on h_s and R. These bins are defined in Table 1, which also gives the total number of observations that went into each bin, summed over the five zones, for the 10 Decembers 1981–90. Bins 12 and 11 represent daylight and twilight. Bins 0–10 represent the night sky; the case of the moon below the horizon at night is bin 0. The bin boundaries for the nighttime moonlit cases were selected to give approximately equal numbers of observations in each bin and to provide appropriate resolution of R.

3. Analysis of moonlit cloud observations

a. *Total cloud cover and clear-sky frequency*

Average total cloud cover (A_c) and clear-sky frequency were computed for each bin for each of the

TABLE 1. Number of observations, average total cloud cover (A_c), and frequency of clear sky (Clear), for December 1981–90, 0°–50°N, for 13 categories of illumination. The values given for A_c and Clear are the means of five 10° zones, in percent. They are also plotted in Figs. 2 and 3. The relative illuminance R is defined by Eq. (1). Solar elevation angle is h_s.

Categories of illumination		Ocean				Land			
Bin number	Bin definition	Number of obs.	Percent of total obs.	A_c	Clear	Number of obs.	Percent of total obs.	A_c	Clear
12 daylight	$-0.25° \leq h_s \leq 90°$	401 632	53.0	64.9	4.7	2 530 150	44.3	55.3	17.3
11 twilight	$-9° \leq h_s < -0.25°$	43 543	5.7	64.2	4.5	393 020	6.9	50.6	21.5
Night ($h_s < -9°$):									
10	$0.60 < R \leq 1.2$	17 513	2.3	61.9	8.7	130 944	2.3	51.1	26.2
9	$0.43 < R \leq 0.60$	17 265	2.3	63.7	7.3	136 388	2.4	52.3	25.3
8	$0.32 < R \leq 0.43$	16 568	2.2	63.8	7.1	146 244	2.6	51.7	25.0
7	$0.23 < R \leq 0.32$	16 890	2.2	62.6	7.9	154 761	2.7	51.1	25.1
6	$0.16 < R \leq 0.23$	14 052	1.9	61.5	8.3	127 372	2.2	50.5	26.0
5	$0.11 < R \leq 0.16$	11 995	1.6	61.8	7.9	108 441	1.9	50.5	25.7
4	$0.07 < R \leq 0.11$	12 392	1.6	60.4	9.2	111 535	1.9	49.7	26.8
3	$0.03 < R \leq 0.07$	17 358	2.3	59.2	9.3	155 129	2.7	48.8	27.7
2	$0.01 < R \leq 0.03$	14 123	1.9	57.7	10.7	130 216	2.3	47.8	28.9
1	$0.00 < R \leq 0.01$	18 666	2.4	55.6	11.6	174 389	3.0	46.2	30.5
0	$R \leq 0.00$	155 942	20.6	53.0	13.4	1 418 116	24.8	45.2	32.6
All	(bins 0–12)	757 940	100.0			5 716 705	100.0		
Sunlight (including twilight)	(bins 11–12)	445 175	58.7			2 923 170	51.1		
All night	(bins 0–10)	312 765	41.3			2 793 535	48.9		
Light night	(bins 5–10)	94 284	12.5			804 150	14.1		
Dark night	(bins 0–4)	218 481	28.8			1 989 385	34.8		

five zones. In a single month at a single point on the earth, the moon is above the horizon at night for only about 2 weeks, and each category of lunar illuminance is represented by even less time. For this study we therefore chose to average over synoptic and geographical variability by using all observations from 10 Decembers in an entire latitude zone, irrespective of longitude and year, classified only according to the lunar illuminance. (The values obtained are therefore not true zonal averages of cloud cover because the different longitude boxes do not contribute equally according to their areas but rather in proportion to their numbers of observations. True zonal averages of cloud cover will be given below in Table 3 and Fig. 4.) The December averages of A_c within the five latitude zones, as well as the average of these five samples (not area weighted), are plotted against the relative illuminance R in Fig. 2. Daylight values (sun above the horizon) are shown to the right of the figure for comparison.

Each bin in the bold curve in Fig. 2 is represented by at least 11 000 observations for ocean and 108 000 for land (the numbers of observations are given in Table 1). The curves are fairly smooth except for a few excursions that probably result in part from uneven distributions of observations in space and time within a zone. In every zone the brightest bin shows slightly less cloud cover than does the next-brightest bin; this may be due to a true diurnal cycle in cloud cover, since contributions to the brightest bin are more likely to be from around midnight when the full moon reaches its highest altitude.

Figure 2 shows that A_c over the oceans is about 10% greater than over the land for all values of illuminance, but that A_c increases with R in both cases. There is a rapid increase in A_c until $R = 0.11$ and only small changes thereafter as the illuminance increases further toward the value for full moon overhead. We assign the name "light night" to $R > 0.11$, and "dark night" to $R \leq 0.11$ (Table 1). The night-detection bias is apparently larger over ocean than over land. For the five zones the difference between reported cloud cover in the light-night bins and that in the no-moon bin is 6 $\pm$ 2% over land and 9 $\pm$ 1% over the ocean. The average daylight values exceed the light-night values by 4% over land and 2% over ocean, which we think is due to a true diurnal cycle in the regions of greatest data density within the zones used for the analysis. We will see below that the global average day–night differences are less than these values.

The results of the analysis for frequency of clear sky are shown in Fig. 3 for the mean of the five zones. Clear sky is much more frequent over land than over the oceans, and the day–night difference is greater over land as well. In both cases, the reported clear-sky frequency decreases dramatically with increasing illuminance to $R = 0.11$. Over the ocean, clear sky is reported only half as often with $R > 0.11$ as with no moon.

b. A minimum-illuminance criterion

Figure 2 shows that 1) a fairly constant average cloud cover is obtained over a wide range of illuminance; 2)

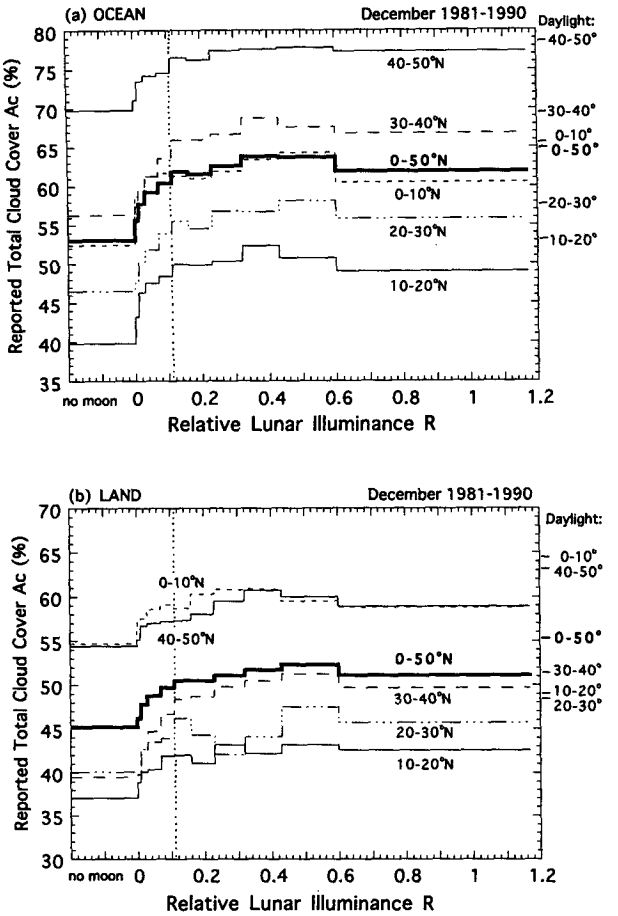

FIG. 2. Reported total cloud cover A_c as a function of relative illuminance R (defined in Eq. 1), for five 10° zones, and their mean value (bold line) for December 1981–90, with the sun more than 9° below the horizon. For comparison, off the right side of the figure is given the average cloud cover when the sun is above the horizon. The illuminance criterion we have chosen based on these data is shown as the vertical line at $R = 0.11$. (a) Ocean. (b) Land.

this average cloud cover is significantly higher than that obtained under no-moon conditions; and 3) there is a rapid transition between these two cases. We conclude that clouds are adequately detected at night by surface observers if the illumination exceeds a threshold value R_c, which we estimate as $R_c = 0.11$. The analyses of total cloud cover (Fig. 2) and clear-sky frequency (Fig. 3) both suggest this same value of R_c. A similar threshold value of $R_c \approx 0.1$ was obtained by S. Klein (1993, personal communication) in an analysis of cloud observations from five ocean weather stations. To refine the choice of R_c we performed the analysis with different choices of bin boundaries (0.10, 0.11, 0.12), and $R_c = 0.11$ appeared to be the best choice. However, uncertainty in the choice of R_c has only a minor effect on the computed average cloud cover because only a small fraction of all observations are in the neighboring bins; changing R_c to 0.07 or 0.16 causes a change of only 0.1%–0.2% in the nighttime average of A_c, or 0.06%–0.1% in the day plus night average. The important thing is to exclude the large number of nighttime observations made when the moon is below the horizon. Similarly, any error in classifying the observations due to the use of Allen's approximate fit to the lunar phase function (Fig. 1) instead of a tabulation of Rougier's more exact measured values would have little effect on a cloud climatology.

The criterion we have chosen, $R_c = 0.11$, corresponds to a full moon at $h_m = 6°$ at the average earth–moon distance, or a partial moon at a higher elevation angle. A moon less than half full never satisfies the criterion at any elevation angle.

The necessary illuminance can also be obtained from twilight. Using −12.71 for the apparent visual magnitude of the full moon at its average distance, and −26.80 for that of the sun (Hapke 1971, page 158), the sun is 432 500 times as bright as the full moon. Using the crude assumption that the moon is a gray reflector [actually its albedo is 16% for red light and 9% for blue, according to Table II of Hapke (1971)], then relative values of photometric illuminance can be represented by relative values of radiometric irradiance. Using a solar constant of 1370 W m^{-2} (Hoyt et al. 1992), the irradiance from the full moon at zenith is about 3.2 mW m^{-2}, so $R_c = 0.11$ corresponds to a lunar irradiance of 0.35 mW m^{-2}. This is the same as the irradiance from a twilight sky at $h_s \approx -8.7°$ [according to Fig. 4.4 of Meinel and Meinel (1983)]. This is only an approximate value because of the inexact conversion between photometric and radiometric units, but it agrees with our own visual estimate that the threshold for cloud detection by twilight is at $-9° < h_s < -8°$. For the cloud analysis described below,

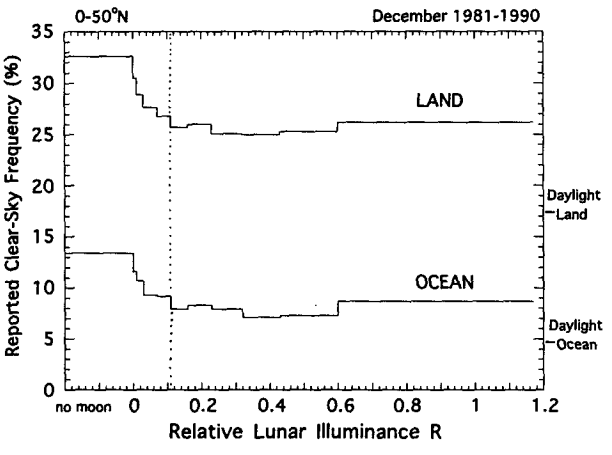

FIG. 3. Reported clear-sky frequency as a function of relative illuminance R for 0°–50°N (mean of five 10° zones) for December 1981–90, with the sun at least 9° below the horizon. For comparison, off the right side of the figure is given the average clear-sky frequency when the sun is above the horizon. The illuminance criterion we have chosen based on these data is shown as the vertical line at $R = 0.11$.

we accept all observations made with either $h_s \geq -9°$ (sunlight or twilight) or $R > 0.11$ (moonlight).

An analysis similar to that in Fig. 2 was performed by Schneider et al. (1989) for the winter observations at the South Pole station, but their plot of A_c as a function of R did not level off as ours does. The lunar altitude rarely exceeds 24° at the South Pole, so R rarely exceeds 0.4, limiting the domain of their analysis. Schneider et al. had a limited sample of data from only one station, and they sorted it into 25 bins of R. Therefore, they had only about 200 observations in each bin, which led to substantial scatter in their results. Our analysis, by comparison, used 10 000–100 000 observations per bin (Table 1). Schneider et al. also apparently did not include the factor $\sin h_m$ in their computation of R in Eq. (1), causing some inaccurate assignment of observations to bins. We performed an analysis of the 800 South Pole synoptic observations that were received on the Global Telecommunications System (GTS) for May–August 1982–91 and obtained results similar to those of Schneider et al.: cloud cover generally increases with R up to about $R = 0.4$, with considerable scatter because of the small number of observations. It was not possible to identify R_c from these results, as they did not exhibit the characteristic leveling off as seen in Figs. 2 and 3. The South Pole observations are now reaching the GTS more reliably than in the 1980s, and this analysis should be redone when more data are available.

4. Effect of an illuminance criterion on computed cloud cover

Application of our illuminance criterion in development of a cloud climatology means that the "dark night" observations are to be discarded. For December in the region 0°–50°N, Table 1 shows that 29% of the ocean reports and 35% of the land reports fall into this category. These same percentages are discarded globally for the season December–January–February (DJF) in our 1982–91 cloud climatology (Hahn et al. 1994). For June–July–August (JJA), only 19% of the reports must be discarded because most land stations and ship reports are made in the Northern Hemisphere, where $h_s > -9°$ for a larger fraction of the time in JJA. Sufficient illumination is provided by either moonlight or twilight for 38% of the observations made with the sun below the horizon in December (Table 1). In the discussions below we sometimes use the term "moonlight criterion" interchangeably with "illuminance criterion" at night.

Using the illuminance criterion, we have computed a 10-yr (December 1981–November 1991) global climatology for total cloud cover, as well as for the frequencies of occurrence of clear sky, fog, and precipitation. We computed averages for 5° × 5° boxes on the same global grid used in W86 and W88. Since there are fewer usable observations made at night than during the day, we formed separate averages for 0600–1800 LT and for 1800–0600 LT, then averaged these two values to obtain the seasonal average. Zonal averages for each season were computed by averaging the boxes within each zone that contained at least 100 observations in the 10 yr for that season. Separate zonal averages were obtained for the land and ocean parts of each zone. Boxes containing both land and ocean were weighted by their fractions of land or ocean in their contributions to the zonal averages. Global averages were obtained by area weighting the zonal averages.

Table 2 gives global averages computed seasonally, both with the sky brightness criterion applied ("light obs") and without ("all obs"), as well as the differences between these two values. Use of the illuminance criterion increases the computed global average total cloud cover by about 2%, and decreases the computed clear-sky frequency by a similar value. Over land the increase in cloud cover is slightly less than the decrease in clear-sky frequency in all four seasons, but over the ocean the increase in cloud cover exceeds the decrease in clear-sky frequency in all four seasons. This implies that, over the ocean, not only is the reported frequency of occurrence of cloud greater under moonlight, but the amount when present is also greater. The evidence

TABLE 2. Global averages (in percent) for total cloud cover and for frequency of clear sky. Seasonal averages for 1982–91 are computed for land and ocean, both with and without the illuminance criterion ("light obs" and "all obs" respectively). Abbreviations for seasons: December–January–February (DJF); March–April–May (MAM); June–July–August (JJA); September–October–November (SON).

		Total cloud cover	Clear sky
DJF land	light obs	54.9	21.3
	all obs	52.9	23.7
	difference	2.0	−2.4
DJF ocean	light obs	68.3	3.1
	all obs	66.1	4.3
	difference	2.2	−1.2
MAM land	light obs	54.8	19.2
	all obs	52.7	22.2
	difference	2.1	−3.0
MAM ocean	light obs	67.7	3.4
	all obs	65.5	4.5
	difference	2.2	−1.1
JJA land	light obs	52.1	21.7
	all obs	50.6	23.7
	difference	1.5	−2.0
JJA ocean*	light obs	69.3	3.2
	all obs	67.3	4.1
	difference	2.0	−0.9
SON land	light obs	53.8	20.9
	all obs	51.9	23.2
	difference	1.9	−2.3
SON ocean	light obs	68.3	3.0
	all obs	66.5	4.1
	difference	1.8	−1.1

* Insufficient ship data were available in JJA to form zonal averages south of 55°S, so estimated values for that region were used in forming the JJA ocean averages.

in Table 2 is insufficient to draw such a conclusion over land.

Table 3 compares zonal averages of total cloud cover computed with and without the illuminance criterion. The values from our earlier surface-based climatologies (W86 and W88) are also given. Since the climatologies of W86 and W88 terminate in 1981, differences between the "all" column and the W88 or W86 column indicate changes in average cloud cover from the earlier span of years to the 1982–91 decade. The ocean averages show generally an increase relative to the earlier span of years, consistent with the trends reported in W88. Comparison of the "all" column with the "light" column shows the effect of applying the illuminance

TABLE 3. Zonal average total cloud cover (%) for 1982–91 computed with and without application of the illuminance criterion ("light" observations and "all" observations, respectively) and compared to the climatologies of W86 and W88. Mean values for two seasons are given for 5° zones and for the two hemispheres and the globe. The 1982–91 results are also plotted in Fig. 4.

	DJF, ocean			DJF, land			JJA, ocean			JJA, land		
	1952–81	1982–91		1971–81	1982–91		1952–81	1982–91		1971–81	1982–91	
	W88	All	Light	W86	All	Light	W88	All	Light	W86	All	Light
Globe	65	66	68	53	53	55	66+	67+	69+	51	51	52
Northern Hemisphere	61	63	65	50	50	52	66	67	69	56	55	56
Southern Hemisphere	68	69	70	59	59	60	66+	68+	70+	42	42	44
50°N–50°S	61	62	65	51	50	52	62	63	66	47	46	48
85°–90°N	47	53	61	—	—	—	82	83	83	—	—	—
80°–85°N	50	57	61	43	44	52	85	81	81	68	69	69
75°–80°N	61	67	71	46	47	52	85	82	82	78	76	76
70°–75°N	66	65	70	50	54	57	80	78	78	73	71	71
65°–70°N	80	79	80	54	56	58	80	80	81	69	69	69
60°–65°N	79	81	82	61	63	65	78	80	80	68	68	68
55°–60°N	80	81	82	64	66	68	81	80	80	66	66	67
50°–55°N	80	81	83	60	62	64	85	85	86	61	61	63
45°–50°N	79	79	81	57	57	59	84	85	86	52	52	54
40°–45°N	75	75	78	55	53	55	74	75	77	46	45	47
35°–40°N	71	72	74	53	51	54	62	65	67	40	40	42
30°–35°N	66	67	70	45	43	47	57	59	61	39	38	40
25°–30°N	60	60	63	34	33	35	54	56	58	35	35	36
20°–25°N*	52	53	56	30	30	32	55	56	59	43	40	41
15°–20°N*	48	49	52	34	33	34	60	61	64	56	51	51
10°–15°N	49	51	54	40	46	47	62	64	67	69	70	72
5°–10°N	59	59	62	48	47	49	69	69	71	75	73	75
0°–5°N	61	62	65	62	60	62	60	61	64	71	69	71
0°–5°S	55	58	62	71	71	73	52	55	59	61	61	62
5°–10°S	57	59	62	74	72	74	55	57	60	44	43	44
10°–15°S	58	60	62	76	73	76	56	57	60	32	31	33
15°–20°S	58	59	62	66	65	67	57	58	61	28	28	30
20°–25°S*	58	59	62	54	53	55	58	59	62	30	28	29
25°–30°S*	59	60	63	41	41	42	60	62	65	33	31	33
30°–35°S	62	63	65	41	41	42	64	64	66	45	46	48
35°–40°S	68	68	69	46	45	47	67	69	71	58	57	60
40°–45°S	74	74	74	54	51	52	72	74	75	61	59	61
45°–50°S	80	78	78	61	60	62	74	76	76	62	59	63
50°–55°S	84	84	84	74	71	72	80	80	82	64	61	64
55°–60°S	88	87	88	88	87	87	—	—	—	84	79	83
60°–65°S	90	90	90	85	84	84	—	—	—	67	75	78
65°–70°S	88	85	85	69	68	69	—	—	—	64	63	66
70°–75°S*	88	83	83	54	56	56	—	—	—	54	50	52
75°–80°S*	77	78	78	48	47	47	—	—	—	43	45	50
80°–85°S	—	—	—	—	—	—	—	—	—	—	—	—
85°–90°S	—	—	—	51	58	58	—	—	—	33	35	37

+ Insufficient ship data are available in JJA to form ocean zonal averages south of 55°S, according to our criterion of 100 observations per box. The few observations that were available were used to estimate an average value of 86% cloud cover for the Southern Ocean south of 55°S, which entered into the computation of Southern Hemisphere and global averages. This value represents 9% of the global ocean area.

* Land boxes with no stations in the Sahara, Western Australia, and Antarctica were given values from their neighbors in computing the zonal average, as described in W86.

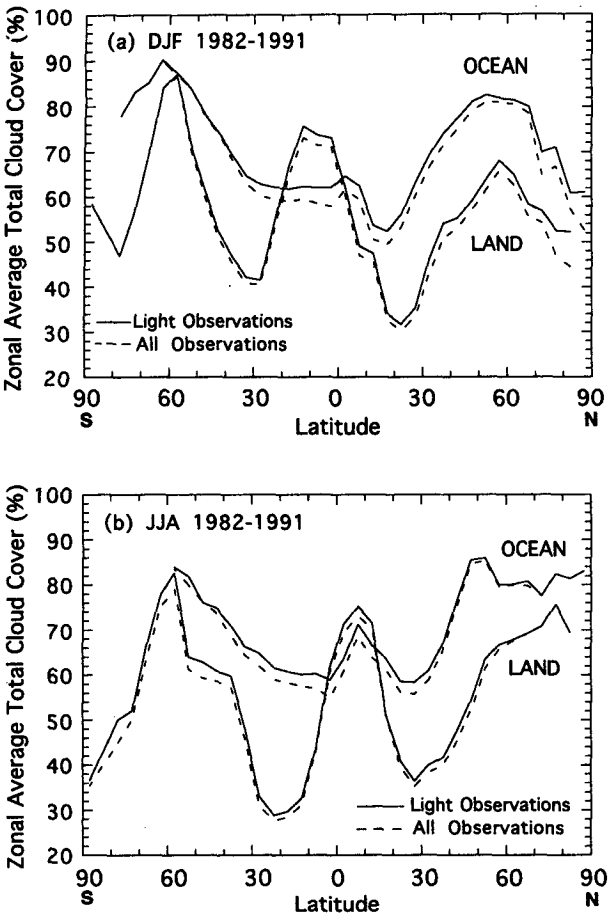

FIG. 4. Zonal average total cloud cover (day + night average) for 5° zones, computed using either all observations or with application of the illuminance criterion ("light" observations). Separate averages are formed for the land and ocean parts of each zone. (a) December–January–February 1982–91. (b) June–July–August 1982–91.

criterion. The "all" and "light" values in Table 3 are graphed in Fig. 4, which shows that the effect of imposing an illuminance criterion is greater in winter than in summer because of the fewer hours of darkness in summer. The largest effect is in the Arctic winter, where the difference is as much as 8%. The polar summers show no difference because the sun is above the horizon most of the time.

Figure 4 also shows some generally recognized aspects of the global distribution of cloud cover: (a) the average cloud cover is less over land than over ocean; (b) the latitudinal variation of cloud cover is greater over land than over ocean; and (c) the peak cloudiness in the intertropical convergence zone moves from 7°N in JJA to only 2°N in DJF over the ocean, but to as far as 12°S over land.

5. Diurnal cycle of cloud cover

Much more dramatic than the 2% increase in seasonal average cloud cover is the effect on computed diurnal cycles when a moonlight criterion is imposed on nighttime observations. We illustrate the effect with some results from our 10-yr climatology, which is available as a data archive (Hahn et al. 1994).

Diurnal cycles were computed for grid boxes of 10° latitude × 20° longitude for the ocean and 5° × 5° for land. In each grid box in each season, average values of cloud cover were obtained for each of the eight synoptic times spaced three hours apart, or four times spaced six hours apart if there were insufficient observations at the intermediate three-hourly times. The four or eight values of A_c were fitted by a cosine curve, whose amplitude and phase are given in Figs. 5 and 6 for two seasons. We display only the ocean results here because they are on a conveniently coarse grid. Comparison of these figures to maps 114 and 115 of W88 shows some differences. Figure 5 shows that during DJF the maximum cloud cover over most of the ocean occurs at night or in the morning, especially in regions far from land, whereas in our earlier work without the moonlight criterion, the computed time of maximum in most regions was near noon. During JJA (Fig. 6), however, afternoon maxima are found over the western parts of the tropical North Pacific and North Atlantic Oceans and over the Arabian Sea and tropical Indian Ocean. These maxima occur slightly later in the afternoon than those given in map 115 of W88. Also, the morning maxima over the eastern tropical oceans and most other ocean regions are slightly earlier than shown in W88. The largest amplitudes are found in the stratocumulus regions of the eastern subtropical oceans, where the maximum cloud cover is reached shortly before sunrise, as was also found from geostationary satellite observations by Minnis and Harrison (1984) and Minnis et al. (1992). In the western equatorial Pacific, 10°N–10°S, where deep cumulonimbus convection is common, we obtain maximum cloud cover generally in the morning, but with some boxes showing afternoon maxima. Fu et al. (1990) obtained a maximum of deep convective clouds in this region in the early morning. Here there are many cloud types contributing to the total cloud cover, so a detailed comparison in this region awaits analysis of the surface observations by cloud type.

Sample diurnal cycles from individual land and ocean boxes for two seasons are shown in Figs. 7–10. The diurnal cycle is shown both with and without imposition of the moonlight criterion and is compared to the three-hourly cloud cover reported for these boxes by the International Satellite Cloud Climatology Project (ISCCP) (Rossow and Schiffer 1991). The ISCCP archive (Rossow et al. 1991) gives values for 2.5° × 2.5° boxes; we averaged together the values from four ISCCP boxes to compare with one 5 × 5 box, or from 32 ISCCP boxes to compare with one 10 × 20 box. The ISCCP averages are for the years 1984–90, but for the surface-based diurnal cycle we used all 10 years, 1982–91, to get better statistical accuracy, since

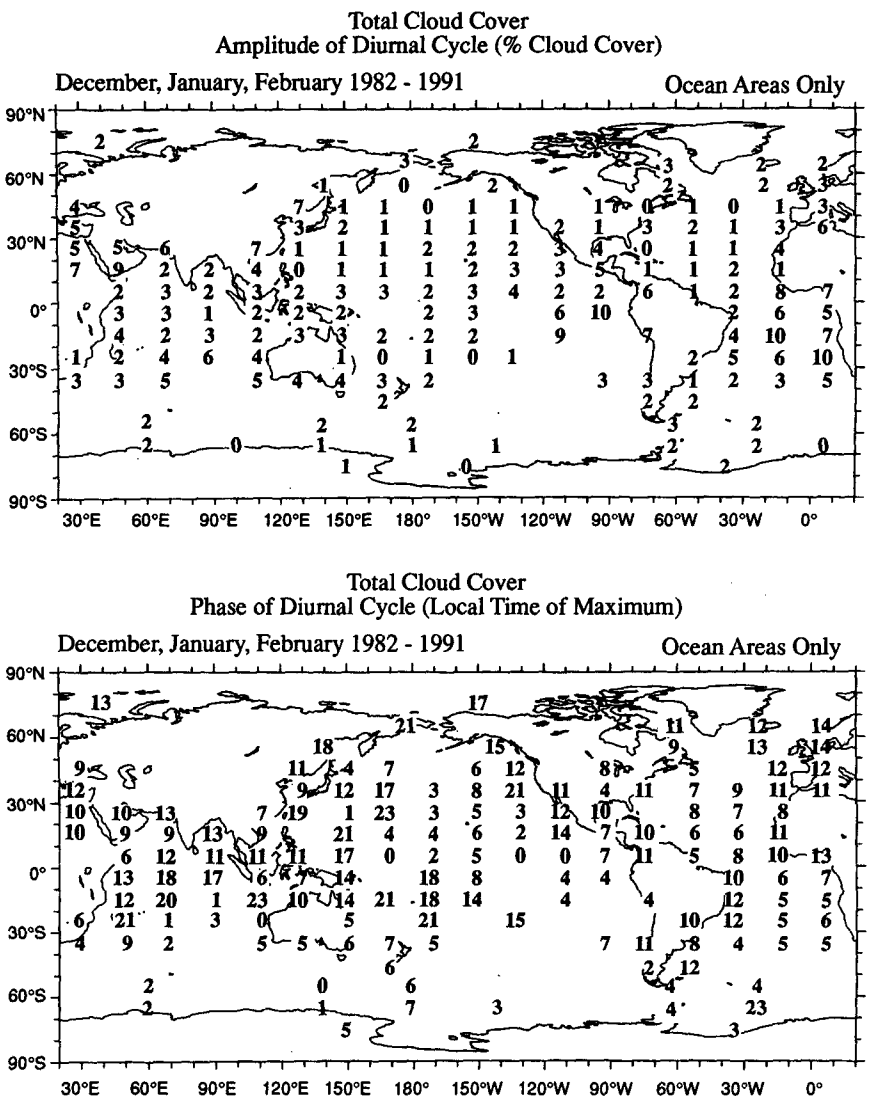

FIG. 5. Average diurnal cycle of total cloud cover for December–January–February 1982–91 using surface observations that satisfied the illuminance criterion. A cosine function was fitted to the eight 3-h averages (or four 6-h averages); the amplitude and phase of that function are given here. The range of the 3 h averages may be more or less than twice the amplitude given here, because the data points may not fit exactly to a cosine function. The phase of the diurnal cycle is given only if the amplitude is at least 1%. In grid boxes that contain both land and ocean, the numbers are printed in the centers of their boxes but apply only to the ocean parts of the boxes. The boxes have longitudinal width 20° for 0°–50° latitude, 40° for 50°–70° latitude, and 60° for 70°–80° latitude.

the ground-based climatology in many places suffers from a scarcity of observations. The ISCCP-C2 data we used were the "adjusted" mean frequency of cloud pixels [i.e., variable 8 in Table 2.3 of Rossow et al. (1991), Appendix C]; the adjustments applied by ISCCP were to correct for a night-detection bias in the satellite data and for any inadequacy in diurnal sampling.

For display in Figs. 7–10 we chose grid boxes that contained sufficient observations, contained exclusively land or ocean, represented different climatic regions, and had exhibited a significant diurnal cycle of A_c in our previous work. In some cases the diurnal cycle disappeared when we imposed the moonlight criterion. The grid-box numbers used in our data archives (Hahn et al. 1988; Hahn et al. 1994) are indicated on the figures for reference. For the ocean (Figs. 7 and 8), 10° × 20° boxes are used, as was done by W88. Even with these large boxes there may not be a sufficient number of observations in the 3-h time periods (0300, 0900, 1500, 2100 UTC), or, more commonly, the number of observations in these time periods is only

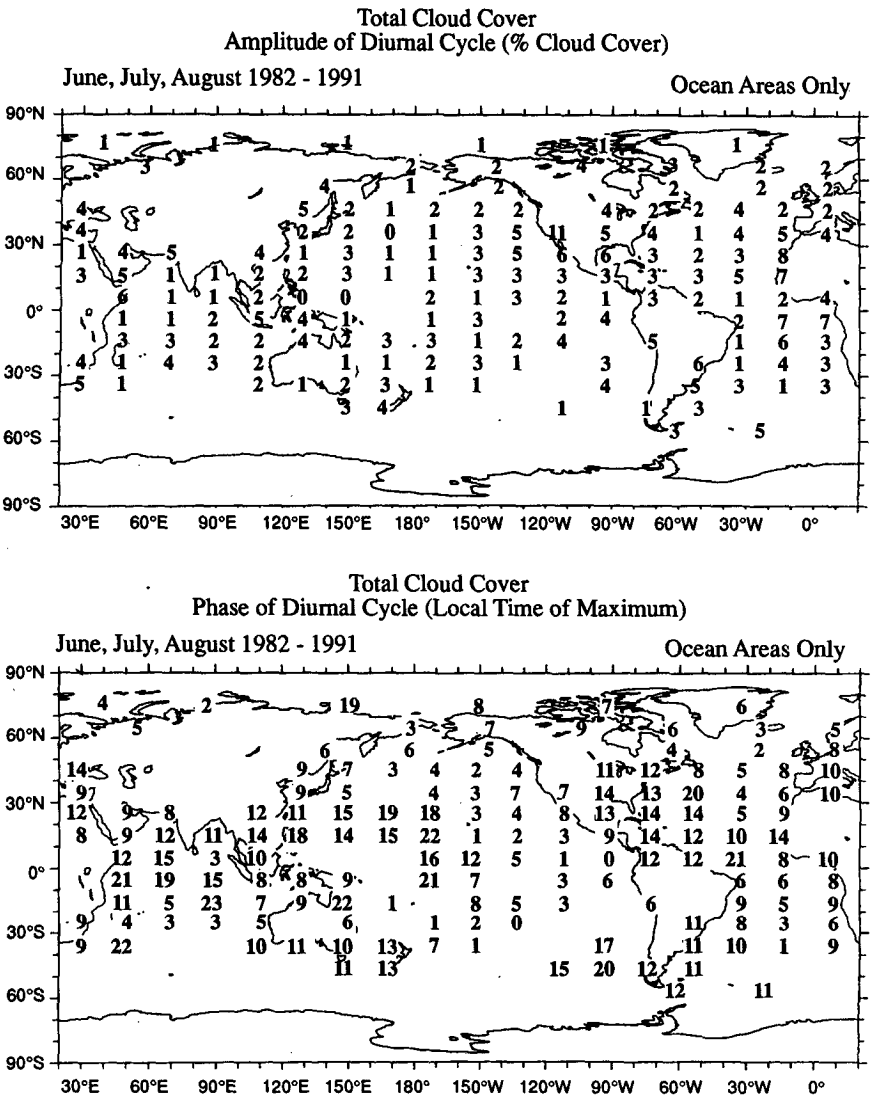

FIG. 6. Same as Fig. 5 but for June–July–August.

a small fraction of the number at the 6-h times (0000, 0600, 1200, 1800 UTC) and thus may not represent comparable data as discussed by W88. Therefore, only data for the 6-h times are plotted. Since land stations are fixed and almost always give a report for their specified reporting times (whether 8, 4, or fewer times per day), the number of observations in a grid box on land usually is more than adequate for our analysis, if the box contains a station. Here we use the 5° × 5° grid used by W86, but data on a 2.5° × 2.5° grid are available in our data archive (Hahn et al. 1994). Most land stations make observations eight times per day; diurnal cycles can therefore be resolved better in time than they can over the ocean. Within a 5° box there are usually several stations (map 1 of W86).

In the North Atlantic in winter (Figs. 7a,b), an apparent diurnal cycle with a maximum near noon disappears when the moonlight criterion is applied. In the eastern North Pacific (Fig. 7c), a small diurnal cycle with a nighttime maximum appears spuriously as a midday maximum if all observations are used. The diurnal amplitude (and phase, when the amplitude is significant) from ISCCP is in rather good agreement with the surface observations using the moonlight criterion. The average value from ISCCP, however, is 10% higher in these regions, which have predominantly stratiform clouds at all levels (Figs. 7a–c). The ISCCP average is lower in the equatorial Atlantic (Fig. 7d) where convective clouds are more common (Map 167a of W88). Surface observers are known to overestimate the coverage of scattered cumulus (but probably by only about 1%, according to Table 8c of W88), and satellites may fail to detect small clouds that occupy only a small fraction of a pixel.

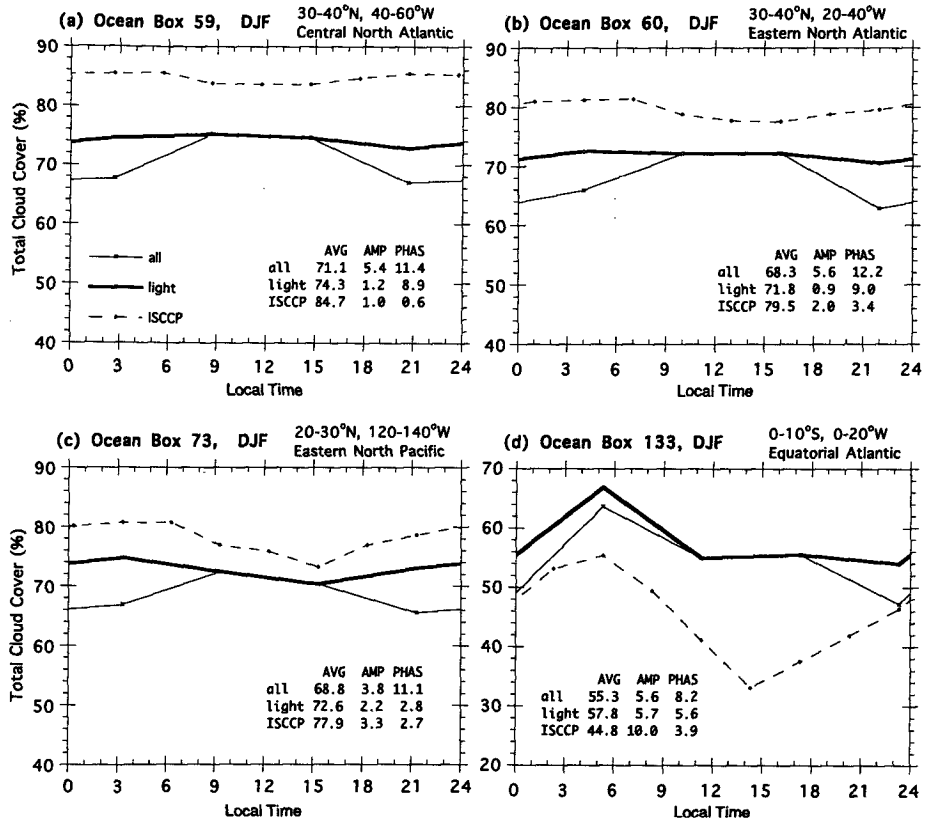

FIG. 7. Sample diurnal cycles of total cloud cover in selected grid boxes over the ocean with large numbers of observations for December–January–February 1982–91. Thick solid lines depict averages for "light" observations; thin solid lines for all observations. Data points are from the six-hourly synoptic times. Grid-box size is 10° lat × 20° long. The average (AVG) of all synoptic times, along with amplitude (AMP) and phase (PHAS; local time of maximum) of a fitted cosine function are given. The diurnal cycle reported by ISCCP for the years 1984–90 is also shown for comparison, with data points for the three-hourly synoptic times.

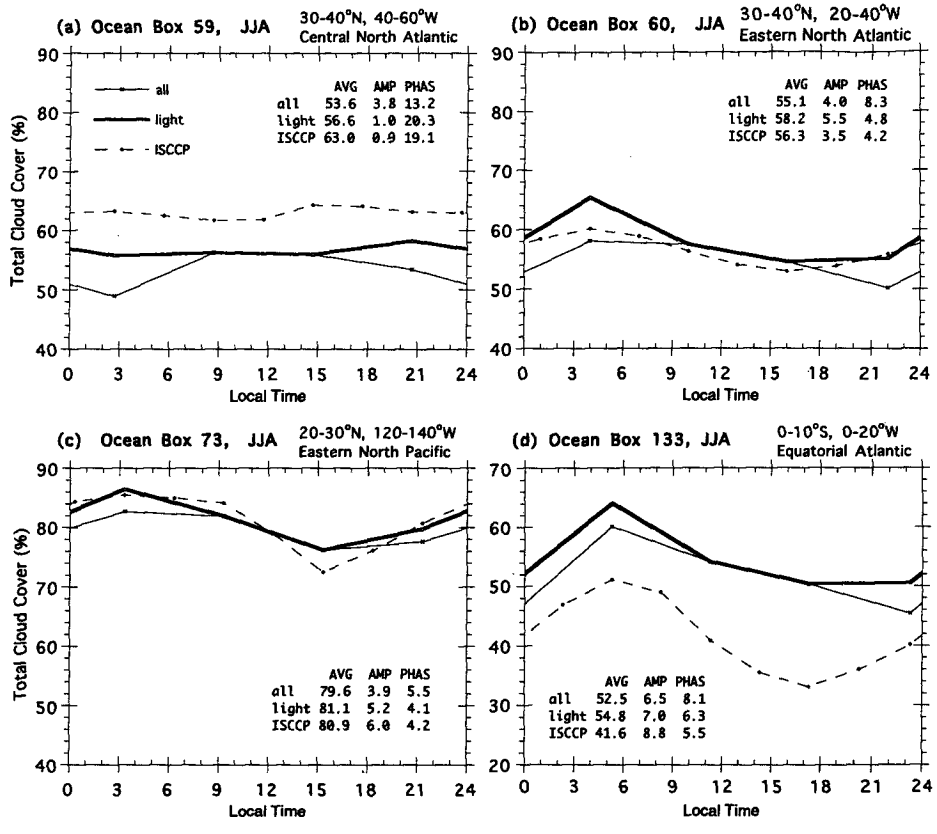

FIG. 8. Same as Fig. 7 but for June–July–August.

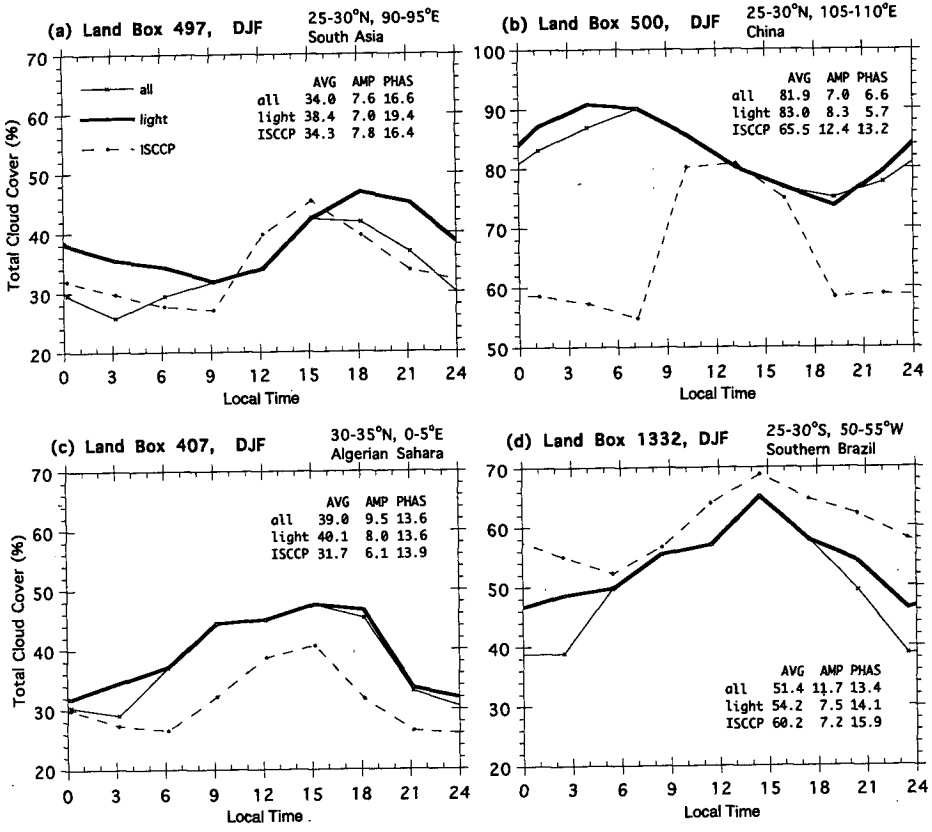

FIG. 9. Sample diurnal cycles for total cloud cover in selected grid boxes over land for December–January–February 1982–91. Grid-box size is 5° lat × 5° long; a grid box may contain several stations. Symbols and line codes are the same as in Fig. 7.

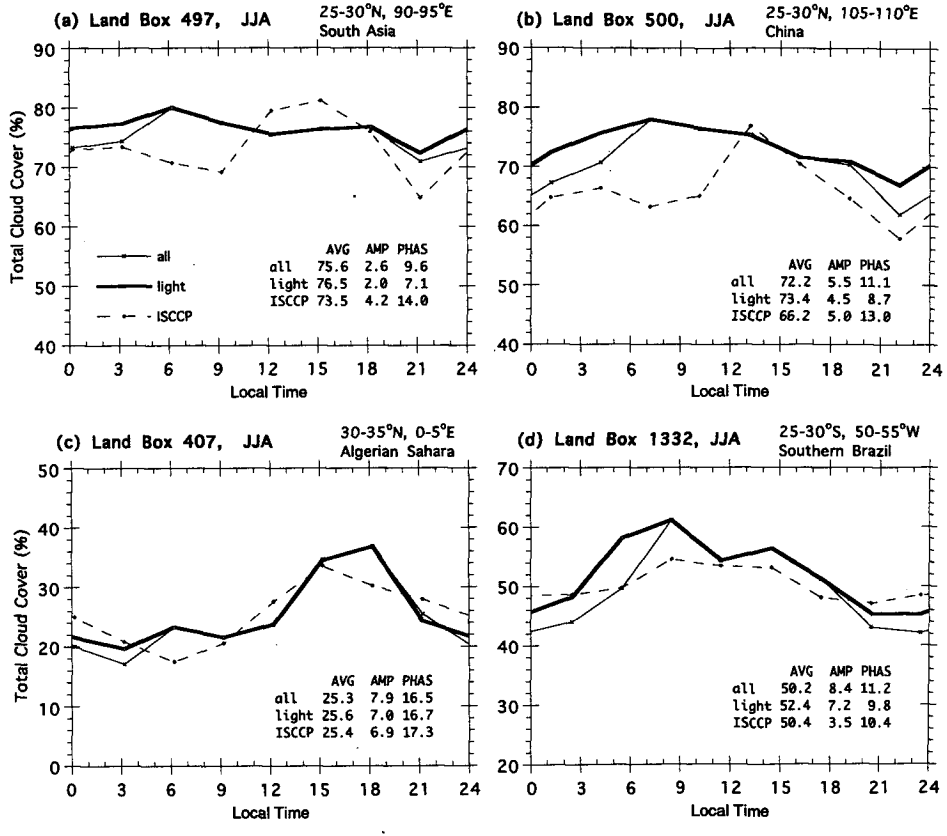

FIG. 10. Same as Fig. 9 but for June–July–August.

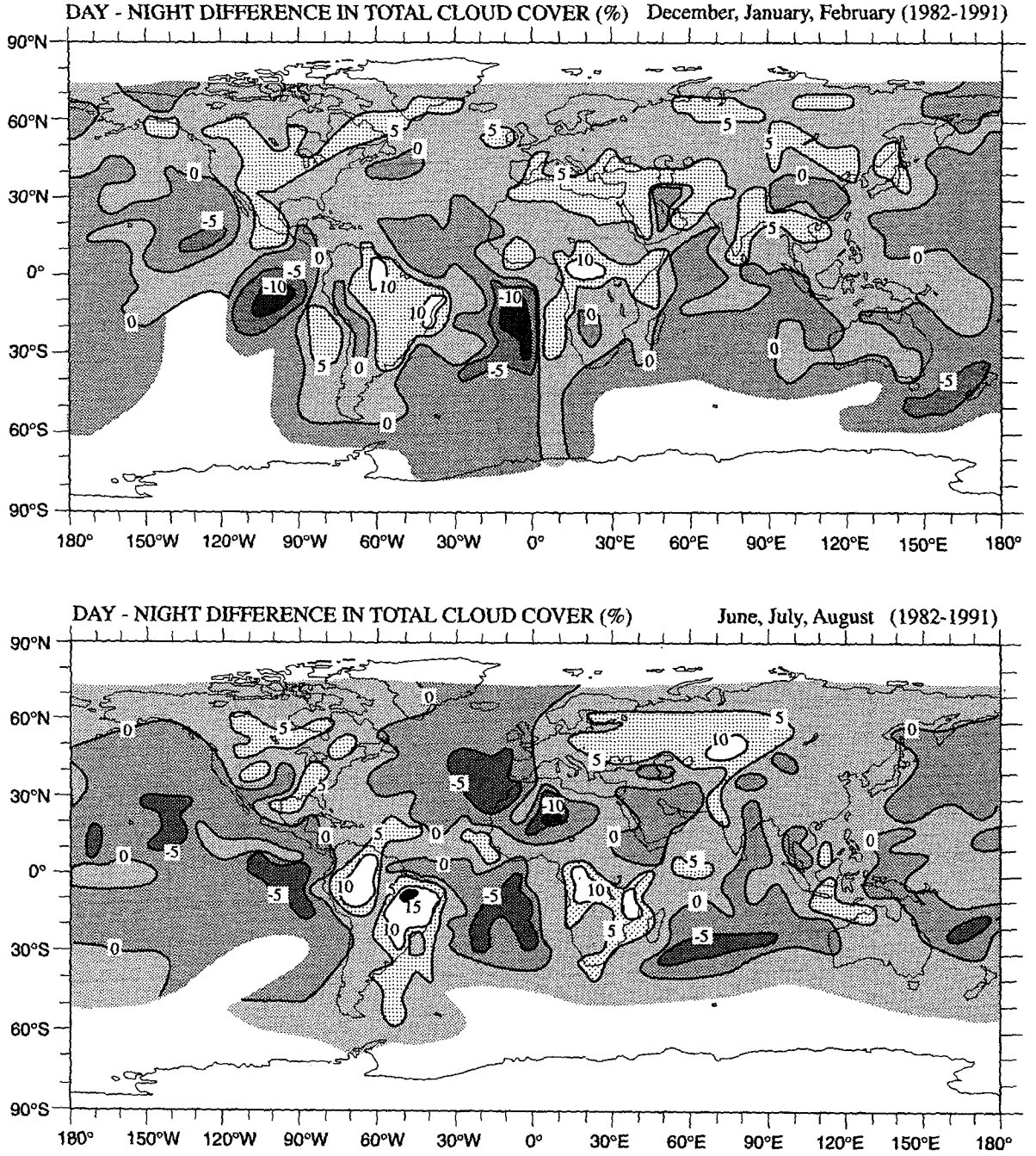

FIG. 11. Difference in percent total cloud cover between day (0600–1800 LT) and night (1800–0600 LT). Values for both land and ocean, on a 5° grid, were contoured by hand, with some smoothing and interpolation. (a) December, January, February. (b) June, July, August. Dark shading means night > day; light shading means day > night.

Figure 8 shows these same ocean boxes for JJA. The diurnal cycles with the moonlight criterion agree better with ISCCP than do those obtained from all observations, but there are still large differences in the averages at two of the locations. Figure 8a is another example of a spurious diurnal maximum near noon that disappears when the moonlight criterion is applied. The North Atlantic (Figs. 8a, b) is less cloudy in summer than in winter. The eastern North Pacific (Figs. 7c and 8c) is cloudier in summer (JJA) than in winter (DJF),

TABLE 4. Hemispheric and global average annual and seasonal total cloud cover, 1982–91, from surface observations screened by the illuminance criterion. Difference between day (0600–1800 LT) and night (1800–0600 LT) is given in parentheses. Estimated values were used for the ocean south of 55°S in JJA.

	Land	Ocean	Land and ocean
	Annual		
Globe	53.9 (3.3)	68.4 (0.3)	64.0 (1.3)
Northern Hemisphere	54.5 (3.2)	66.3 (0.4)	61.5 (1.5)
Southern Hemisphere	52.7 (3.4)	69.9 (0.3)	66.6 (1.0)
50°N–50°S	50.1 (3.8)	64.8 (0.3)	60.8 (1.3)
	December, January, February		
Globe	54.9 (3.7)	68.3 (0.2)	64.3 (1.3)
Northern Hemisphere	52.3 (4.3)	65.5 (1.2)	60.1 (2.4)
Southern Hemisphere	60.3 (2.5)	70.4 (−0.5)	68.4 (0.1)
50°–50°S	52.3 (4.4)	64.7 (0.2)	61.3 (1.3)
	March, April, May		
Globe	54.8 (3.4)	67.7 (0.6)	63.8 (1.5)
Northern Hemisphere	54.7 (3.1)	64.7 (−0.2)	60.6 (1.1)
Southern Hemisphere	55.1 (4.0)	69.8 (1.4)	67.0 (1.9)
50°N–50°S	52.4 (4.0)	64.0 (0.8)	60.9 (1.6)
	June, July, August		
Globe	52.1 (2.7)	69.3 (0.6)	64.1 (1.2)
Northern Hemisphere	56.2 (2.0)	68.7 (−0.2)	63.6 (0.6)
Southern Hemisphere	43.5 (4.1)	69.7 (1.2)	64.6 (1.8)
50°N–50°S	47.6 (2.7)	65.6 (0.6)	60.7 (1.1)
	September, October, November		
Globe	53.8 (3.5)	68.3 (−0.2)	63.9 (0.9)
Northern Hemisphere	54.8 (3.7)	66.3 (0.8)	61.6 (2.0)
Southern Hemisphere	51.7 (3.0)	69.8 (−0.9)	66.2 (−0.2)
50°N–50°S	48.1 (3.8)	64.7 (−0.1)	60.2 (1.0)

as is the south equatorial Atlantic, where summer is DJF (Figs. 7d and 8d). At both of these locations larger cloud amounts are obtained at night with the moonlight criterion, but the computed amplitude and phase in JJA do not change by much. The early morning maximum is found in both winter and summer in the eastern North Pacific (Figs. 7c and 8c), whereas W88 (maps 114b and 115b) reported a 6-h shift in phase from summer to winter, which was a spurious result of the night-detection bias.

Figures 9 and 10 illustrate diurnal cycles over land. In the Assam–Bangladesh region in DJF (Fig. 9a) the moonlight criterion has a large effect on A_c at night, but causes little change to the amplitude or phase because the maximum occurs near sunset. In a mountainous region of southwestern China (Fig. 9b) there is good agreement with ISCCP during the day but poor agreement at night. Agreement is somewhat better in the summer (Fig. 10b). About 26 stations contribute to this box, so its subbox geographical variations are probably sampled adequately. In this box there is a large amount of nimbostratus in winter (23%; Map 136 of W86), with strong horizontal gradients of amount in every direction.

In the Algerian Sahara and southern Brazil (Fig. 9c, d) the maximum cloud cover occurs in midday, so application of the moonlight criterion causes a reduction in the diurnal amplitude but little change in phase. The average A_c reported by ISCCP in the Saharan box agrees with the surface observations in JJA (Fig. 10c) when the predominant clouds are altostratus and altocumulus, but is 8% lower than the surface observations in winter (Fig. 9c) when the predominant type is cirriform and, therefore, probably thinner. In southern Brazil the average A_c from ISCCP is higher than that from surface observations in the wet season (Fig. 9d) but lower in the dry season (Fig. 10d); the reason is unclear.

The Indian monsoon causes a large seasonal cycle north of the Bay of Bengal. The average cloud cover

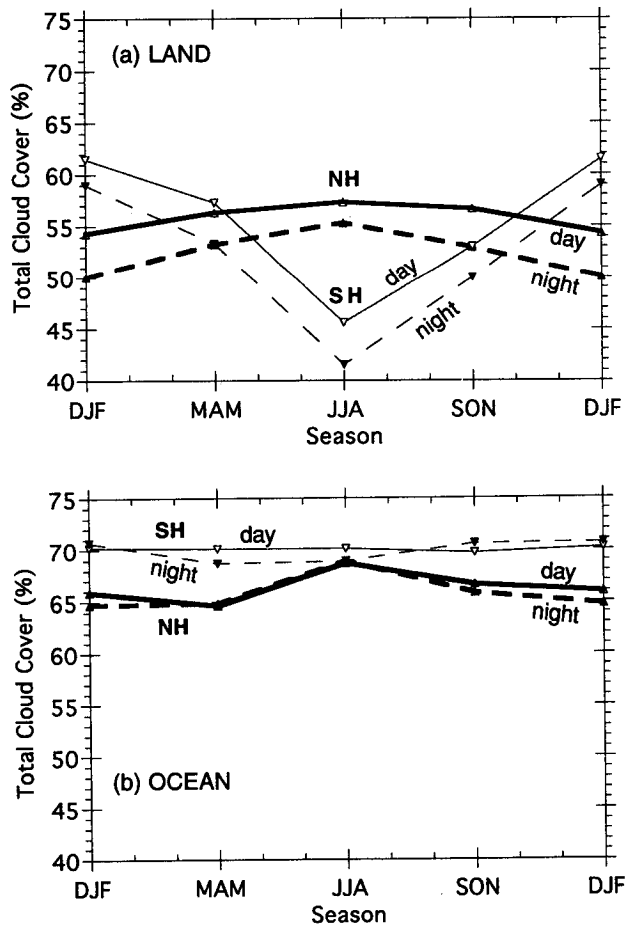

FIG. 12. Seasonal cycles of hemispheric-average cloud cover for day (0600–1800 LT, solid lines) and night (1800–0600 LT, dashed lines), for the years 1982–91, using observations screened by the illuminance criterion. (a) Land. (b) Ocean.

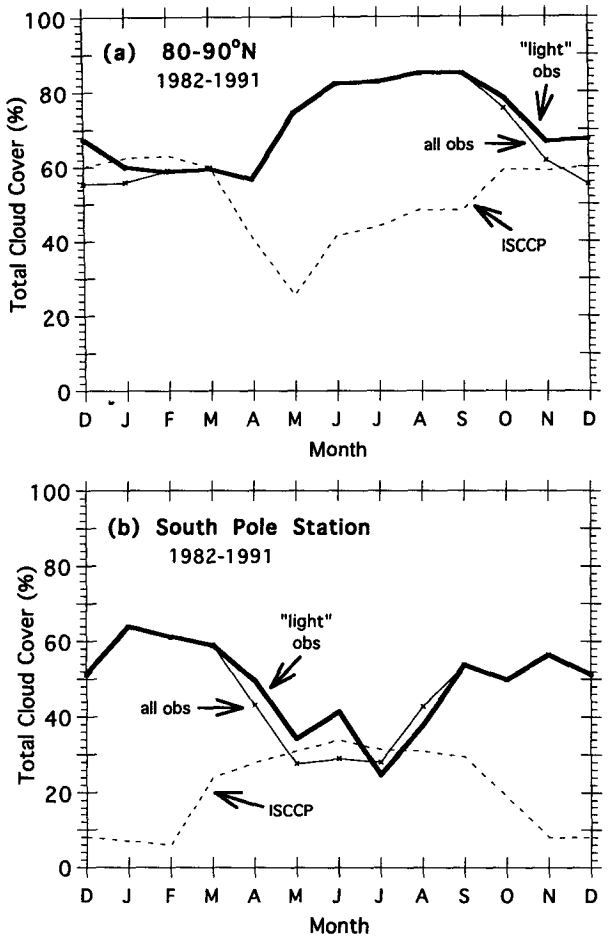

FIG. 13. Seasonal cycle of total cloud cover in the polar regions for 1982–91 obtained from surface observations with and without application of the illuminance criterion ("light" and "all," respectively). The two datasets are identical in summer when the sky is sunlit throughout each month and disagree in winter when the sky is moonlit only part of each month. Zonal average cloud cover from ISCCP for 1983–91 for the latitude zones 80°–90°N and 80°–90°S are also shown; they are taken from Rossow et al. (1993). (a) Average cloud cover was obtained from all observations from ships and ice islands in the zone 80°–90°N. The winter values shown here, both with and without the moonlight criterion, are higher than those for 1952–81, as discussed in the text. (b) Average cloud cover was obtained from surface observations made only at the South Pole station (90°S). Only a small fraction of the winter observations reached the GTS, so the winter values plotted here are rather uncertain. The data points for "light" observations in April–August are unreliable; each is an average of only about 60 observations.

is only 38% in DJF (Fig. 9a), but 76% in JJA (Fig. 10a). The diurnal cycle in JJA from ISCCP is much larger than that seen from the surface (Fig. 10a). It may be that ISCCP detects cumulonimbus in the late afternoon more readily than cirrus in the morning. However, definitive explanation of these differences cannot be attempted until diurnal cycles have been analyzed for the individual cloud types. The one important result that is common to all eight locations in both seasons in Figs. 7–10 is that the average cloud cover reported at night is in every case higher with the aid of moonlight.

6. Difference between daytime and nighttime cloud cover

In Fig. 11 we divide the 24-h period everywhere into two equal parts and display the difference in total cloud cover between "day" (0600–1800 LT) and "night" (1800–0600 LT) for two seasons. For this figure, the 5° × 5° values for both land and ocean were contoured by hand, with some smoothing and interpolation.

Most of the continents have greater cloud cover during the day, the west coasts of North and South America in their summer seasons being notable exceptions. The regions where cloud cover is greater at night are predominantly in the open oceans far from land and particularly during summer. Over the low-latitude oceans, however, there is a tendency for greater cloud cover during the day, especially over the western parts of the tropical oceans. At higher latitudes in the Northern Hemisphere, cloud cover in winter is slightly greater during the day than at night over most of the North Atlantic and part of the North Pacific. But in summer, the cloud cover is greater at night, probably because the predominant nighttime overcast stratus decks become broken during daylight hours. An analogous situation occurs for the Southern Hemisphere oceans. There are also a few exceptions to the general pattern of greater daytime cloud cover over land. In the central United States, the Sahara, Arabia, and Southwest Africa, there is a nighttime maximum of total cloud cover during the summer. In the central United States, this is consistent with the nocturnal maximum of summer thunderstorms (Pitchford and London 1962; Wallace 1975).

The results in Fig. 11 are summarized in Table 4 as global and hemispheric averages. Insufficient ship data were available to form zonal averages for the ocean south of 55°S in JJA (according to our criterion of 100 observations per box). So in computation of Southern Hemisphere and global averages, estimated values for this region were entered based on the few data that were available. In Table 4 we also present averages for the region 50°N–50°S, covering 77% of the earth's area, for which there was adequate geographical sampling in all seasons.

The global annual average cloud cover of 64.0% from surface observations is close to the 62.6% obtained by ISCCP (Rossow et al. 1993) for essentially the same span of years. The land average of 53.9% exceeds ISCCP's 47.1%, but the ocean average of 68.4% is less than the 70.2% of ISCCP. ISCCP processing is expected to produce a small underestimate of cloud cover over land and a small overestimate over oceans (Rossow et al. 1993). We find that the average cloud cover from surface observations is greater during the day than at

night, by 3.3% over land but only 0.3% over the oceans. By comparison, the ISCCP results show a day–night difference of +4.5% over land and −2.1% over oceans [using ISCCP's "corrected" nighttime data; Table 3 of Rossow et al. (1993)].

7. Seasonal cycle of hemispheric daytime and nighttime cloud cover

Figure 12 displays the seasonal cycles of hemispheric averages. The seasonal cycles are much larger over land and exhibit summer maxima in both hemispheres for both day and night, with daytime values exceeding nighttime values by 3%–4%. The Northern Hemisphere (NH) ocean (Fig. 12b) also shows a summer maximum with little difference between day and night. The Southern Hemisphere (SH) ocean shows a very small seasonal cycle at night but none during the day. By contrast, the SH land areas show a large seasonal variation, larger than NH land areas. This is because most of the SH land is in the Tropics and subtropics where JJA is the dry season, whereas the NH land is mostly in the middle latitudes.

For all four cases shown in Fig. 12 (NH and SH, land and ocean), the day–night difference is slightly larger in autumn and winter, the two darkest seasons. We consider this to represent a true seasonal difference in diurnal cycle, rather than a residual night-detection bias remaining in the screened data. A residual bias would be expected to have a smaller effect on the day–night difference when both "day" (0600–1800 LT) and "night" (1800–0600 LT) are largely dark (winter) or largely light (summer). The largest effect of a residual bias would instead appear in the equinoctial seasons when the "day" and "night" are most different from each other in their illumination. Figure 12 therefore shows no evidence for a residual bias.

8. Seasonal cycle of cloud cover at the poles

In the polar regions, the winter is dark so the *seasonal* cycle can be in error if observations are not screened by a moonlight criterion. In the Arctic Ocean, reports from ships and ice-island camps exhibit a large seasonal cycle with $A_c > 80\%$ in summer and $A_c \approx 50\%$ in winter, as shown in Fig. 3 of Vowinckel (1962) [reproduced as Fig. 11 of Vowinckel and Orvig (1970)]. If we use all observations we obtain similar results, though somewhat higher in winter (Fig. 13a), but the winter values of A_c rise to above 60% if the observations are screened by the moonlight criterion.

Comparison of three surface-based climatologies (*without* screening for moonlight) suggests a recent climatic change in the winter average cloud cover for the central Arctic Ocean (80°–90°N). Vowinckel (1962) used data from 1951 to 1960 and obtained a winter average of 40% at 85°N. Our average (Table 3, for DJF ocean, 80°–90°N) for 1952–81 is 49%, and for 1982–91 is still higher at 56%. None of these climatologies included clear-sky ice-crystal precipitation ("diamond dust," present-weather codes 76 and 78) as clouds, although Curry and Ebert (1992) have argued that diamond-dust layers in the Arctic are often thick enough to have radiative effects comparable with clouds.

We also include the ISCCP seasonal cycles (Fig. 8 of Rossow et al. 1993) in Fig. 13 for comparison. At both poles the ISCCP satellite-derived cloud cover is much lower than that observed from the surface in spring, summer, and autumn, but not in winter. Satellites have particular difficulties detecting clouds over snow because clouds cause less change to both the scene albedo and to the scene brightness temperature over snow than they do over other surfaces (Schweiger and Key 1992; Rossow et al. 1993, section 4d).

At the South Pole station (Fig. 13b), screening of the winter observations by our moonlight criterion causes an increase in the average winter cloud cover but does not raise it to the summer value as Schneider et al. (1989) suggested. Their estimate of South Pole sky cover was based on the intersection of the linear fit to their sky-cover-versus-relative-illuminance data with the maximum illuminance point. This procedure is approximately equivalent to using the average of their brightest bin only (see section 3b). The motivation for Schneider et al.'s work was the suitability of the South Pole for optical astronomy; so the data they analyzed were not the synoptic reports but rather the sky-cover reports, which at the South Pole normally include not just clouds but also other obscurations of the sky, such as blowing snow. This may explain why their estimate of winter sky cover is greater than the winter cloud cover we obtain in Fig. 13b. Nighttime cloud observations on the Antarctic Plateau present special difficulties: 1) the typically thin clouds may cause no more dimming of the stars than does heavy diamond dust; 2) moonlit clouds may be confused with aurora, which is usually colorless and occurs on most days; and 3) obscuration of the sky due to blowing snow can occur nearly one-third of the time in winter and is probably correlated with cloud cover. Because of these peculiarities, it would be appropriate to single out the South Pole cloud climatology for a special study.

9. Diurnal cycles of cloud types

In our earlier work we obtained circumstantial evidence that the night-detection bias was most severe for altostratus, altocumulus, and cirriform clouds (Fig. 9 of W88), so we did not report diurnal cycles for these types in W86 and W88. Use of a moonlight criterion in the analysis of cloud-type amounts will make it possible in future work to obtain diurnal cycles for these types from surface observations. It will then be possible to examine with surface data the conclusions drawn from satellite observations regarding diurnal variations within various cloud levels (e.g., Minnis and Harrison

1984). Minnis and Harrison noted that even where diurnal variations in total cloud cover are small, there may be large diurnal variations of individual cloud types at different levels that tend to cancel each other's contributions to the total cloud cover.

10. Summary and conclusions

This study confirms the existence of a night-detection bias in visual observations of clouds but shows that this bias can be largely eliminated in estimates of climatological-average cloud cover by using only those nighttime observations made at times when sufficient illumination is provided by moonlight or twilight.

The World Meteorological Organization's instructions to observers (WMO 1956, section 5) states that "On nights when the moon is more than one-quarter full, it should be possible to identify clouds and to determine the total cloud cover and the cloud amounts of different types almost as well as in daylight." We come to a similar conclusion, but we would suggest that a somewhat greater level of illumination is necessary. This level of illumination, 11% of that from a full moon overhead at its mean distance from the earth, corresponds to a full moon at 6° above the horizon (at mean distance) and is equivalent to the twilight illumination provided by the sun at about 9° below the horizon. The illuminance criterion is such that a half moon is not quite bright enough to meet the requirement, even at zenith. The illuminance incident on the top of the atmosphere from the moon depends on the moon's phase, its distance from the earth, and its angle above the horizon; these can be determined from an ephemeris.

Ten years of visual observations from stations on land and ships in the ocean have been analyzed for total cloud cover A_c. Average nighttime values of A_c are about 4% greater (and clear-sky frequency about 4% less) with the moonlight criterion imposed than without it, making the global day plus night average A_c about 2% greater (and clear-sky frequency about 2% less).

Computed diurnal cycles are more dramatically affected. Diurnal cycles of total cloud cover over much of the ocean tend to show nighttime or morning maxima rather than the noontime maxima previously published, and average cloud cover is now generally found to be greater at night than during the day over the central oceans far from the continents. Over land, near-noon maxima remain common but amplitudes are reduced. The diurnal amplitude and phase obtained from ISCCP in selected locations agree better with those obtained from surface observations if the moonlight criterion is imposed on the surface observations.

At the North and South Poles, computed seasonal cycles in cloud cover are altered slightly by imposition of the illuminance criterion, but summertime maxima are still found at both poles. This pattern remains in conflict with ISCCP estimates of polar cloud cover.

An archive of the 10-yr climatology (1982–91) sampled here is now available (Hahn et al. 1994) for further studies, such as analysis of trends in nighttime and daytime cloud cover.

Acknowledgments. We thank Richard Stephenson (Physics Department, University of Durham, United Kingdom) for providing his program to calculate positions of the sun and moon, Roy Garstang and Bruce Hapke for discussions about the lunar phase function, Fei Wu for calculating the diurnal cycles from ISCCP, Elizabeth Ebert for the reference to Sverdrup, and Stephen Klein for discussions. Bill Rossow and an anonymous reviewer provided valuable comments on the first draft. SGW thanks the South Pole meteorologists of winter 1992, Kitt Hughes and Bob Koney, for numerous training sessions on how to observe clouds at night, both with and without moonlight. This work was supported by NASA Grant NAG-1-998 and by DOE-ARM (Battelle Contract 144806-A-Q1).

REFERENCES

Allen, C. W., 1973: *Astrophysical Quantities.* 3d ed. Athlone Press, 310 pp.

Bond, D. S., and F. P. Henderson, 1963: *The Conquest of Darkness.* AD346297L, Defense Documentation Center, Alexandria, Virginia, 334 pp.

Curry, J. A., and E. E. Ebert, 1992: Annual cycle of radiation fluxes over the Arctic Ocean: Sensitivity to cloud optical properties. *J. Climate,* **5,** 1267–1280.

Fu, R., A. D. Del Genio, and W. B. Rossow, 1990: Behavior of deep convective clouds in the tropical Pacific deduced from ISCCP radiances. *J. Climate,* **3,** 1129–1152.

Hahn, C. J., S. G. Warren, J. London, R. L. Jenne, and R. M. Chervin, 1988: Climatological data for clouds over the globe from surface observations. Numerical Data Package NDP-026, 54 pp. [Available from Carbon Dioxide Information Analysis Center, MS-050, Oak Ridge National Laboratory, P.O. Box 2008, Oak Ridge, TN 37831-6050.]

——, ——, and ——, 1994: Climatological data for clouds over the globe from surface observations, 1982–1991: Data tape documentation for the total cloud edition. Numerical Data Package NDP-026A, 42 pp. [Available from Carbon Dioxide Information Analysis Center, MS-050, Oak Ridge National Laboratory, P.O. Box 2008, Oak Ridge, TN 37831-6050.]

Hapke, B. W., 1963: A theoretical photometric function for the lunar surface. *J. Geophys. Res.,* **68,** 4571–4586.

——, 1971: Optical properties of the lunar surface. *Physics and Astronomy of the Moon,* 2d ed., Z. Kopal, Ed., Academic Press, 155–211.

Harrison, E. F., P. Minnis, B. R. Barkstrom, V. Ramanathan, R. D. Cess, and G. G. Gibson, 1990: Seasonal variation of cloud radiative forcing derived from the Earth Radiation Budget Experiment. *J. Geophys. Res.,* **95,** 18 687–18 703.

Hoyt, D. V., H. L. Kyle, J. R. Hickey, and R. M. Maschhoff, 1992: The *Nimbus 7* solar total irradiance: A new algorithm for its derivation. *J. Geophys. Res.,* **97,** 51–63.

McCartney, E. J., 1976: *Optics of the Atmosphere.* Wiley, 408 pp.

Meinel, A., and M. Meinel, 1983: *Sunsets, Twilights, and Evening Skies.* Cambridge University Press, 163 pp.

Minnis, P., and E. F. Harrison, 1984: Diurnal variability of regional cloud and clear-sky radiative parameters derived from GOES data. Part II: November 1978 cloud distributions. *J. Climate Appl. Meteor.,* **23,** 1012–1031.

——, P. W. Heck, D. F. Young, C. W. Fairall, and J. B. Snider, 1992: Stratocumulus cloud properties derived from simultaneous

satellite and island-based instrumentation during FIRE. *J. Appl. Meteor.*, **31**, 317–339.

Pitchford, K. L., and J. London, 1962: The low-level jet as related to nocturnal thunderstorms over midwest United States. *J. Appl. Meteor.*, **1**, 43–47.

Radio Corporation of America, 1974: *Electro-Optics Handbook.* Radio Corporation of America, Commercial Engineering Division, Harrison, New Jersey, 225 pp.

Ramanathan, V., R. D. Cess, E. F. Harrison, P. Minnis, B. R. Barkstrom, E. Ahmad, and D. Hartmann, 1989: Cloud-radiative forcing and climate: Results from the Earth Radiation Budget Experiment. *Science*, **243**, 57–63.

Riehl, H., 1947: Diurnal variation of cloudiness over the subtropical Atlantic Ocean. *Bull. Amer. Meteor. Soc.*, **28**, 37–40.

Rossow, W. B., and R. A. Schiffer, 1991: ISCCP cloud data products. *Bull. Amer. Meteor. Soc.*, **72**, 2–20.

——, L. C. Garder, P. J. Lu, and A. W. Walker, 1991: International Satellite Cloud Climatology Project (ISCCP), documentation of cloud data. WMO/TD-266, 76 pp plus 3 appendixes.

——, A. W. Walker, and L. C. Garder, 1993: Comparison of ISCCP and other cloud amounts. *J. Climate*, **6**, 2394–2418.

Rougier, G., 1933: Photométrie photoélectrique globale de la lune. *Annales de l'Observatoire de Strasbourg*, **2**, 3, 203–339.

Schneider, G., P. Paluzzi, and J. P. Oliver, 1989: Systematic error in the synoptic sky cover record of the South Pole. *J. Climate*, **2**, 295–302.

Schweiger, A. J., and J. R. Key, 1992: Arctic cloudiness: Comparison of ISCCP-C2 and *Nimbus-7* satellite-derived cloud products with a surface-based cloud climatology. *J. Climate*, **5**, 1514–1527.

Sverdrup, H. U., 1933: *The Norwegian North Polar Expedition with the "Maud", 1918–1925, Scientific Results.* Vol. 2: *Meteorology, Part I, Discussion.* John Griegs, 331 pp.

Vowinckel, E., 1962: *Cloud Amount and Type over the Arctic.* Vol. 51. *Publications in Meteorology,* McGill University, 64 pp.

——, and S. Orvig, 1970: The climate of the north polar basin. *Climates of the Polar Regions, World Survey of Climatology,* Vol. 14, S. Orvig, Ed., Elsevier, 129–252.

Wallace, J. M., 1975: Diurnal variations in precipitation and thunderstorm frequency over the conterminous United States. *Mon. Wea. Rev.*, **103**, 406–419.

Warren, S. G., C. J. Hahn, J. London, R. M. Chervin, and R. L. Jenne, 1986: Global distribution of total cloud cover and cloud type amounts over land. NCAR Tech. Note TN-273+STR, Boulder, CO, 29 pp + 200 maps.

——, ——, ——, ——, and ——, 1988: Global distribution of total cloud cover and cloud type amounts over the ocean. NCAR Tech. Note TN-317+STR, Boulder, CO, 42 pp. + 170 maps.

Woodruff, S. D., R. J. Slutz, R. L. Jenne, and P. M. Steurer, 1987: A comprehensive ocean–atmosphere data set. *Bull. Amer. Meteor. Soc.*, **68**, 1239–1250.

WMO, 1956: *International Cloud Atlas.* World Meteorological Organization, 62 pp. + 72 plates.